Magnetic Resonance in Medicine 46:1174–1188 (2001)

Theoretical Analysis of the Effects of Noise on Diffusion Tensor Imaging

Adam W. Anderson*

A theoretical framework is presented for understanding the effects of noise on estimates of the eigenvalues and eigenvectors of the diffusion tensor at moderate to high signal-to-noise ratios. Image noise produces a random perturbation of the diffusion tensor. Power series solutions to the eigenvalue equation are used to evaluate the effects of the perturbation to second order. It is shown that in anisotropic systems the expectation value of the largest eigenvalue is overestimated and the lowest eigenvalue is underestimated. Hence, diffusion anisotropy is overestimated in general. This result is independent of eigenvalue sorting bias. Furthermore, averaging eigenvalues over a region of interest produces greater bias than averaging tensors prior to diagonalization. Finally, eigenvector noise is shown to depend on the eigenvalue contrast and imposes a theoretical limit on the accuracy of simple fiber tracking schemes. The theoretical results are shown to agree with Monte Carlo simulations. Magn Reson Med 46: 1174–1188, 2001. © 2001 Wiley-Liss, Inc.

Key words: diffusion tensor; noise; fiber tracking

Diffusion tensor imaging (DTI) is a noninvasive method of characterizing tissue microstructure (1). In simple models of water diffusion in tissues, the directional dependence of diffusion is defined by the diffusion tensor. For example, the directions of highest and lowest diffusion are eigenvectors of the tensor and the diffusion coefficients in these directions are the corresponding eigenvalues. The anisotropy of diffusion in tissues is due primarily to cell membranes (2,3). Hence, the diffusion tensor depends on the cellular structure of tissues. DTI has been used to classify tissues on the basis of diffusion anisotropy (4), characterize changes associated with disease (5–7) and aging (8), and construct three-dimensional models of fiber tracts (9–11).

The diffusion tensor is estimated using a set of diffusion weighted images. Image noise produces errors in the calculated tensor and hence in its eigenvalues (principal diffusivities) and eigenvectors (principal axes). Random variations in these quantities complicate the analysis and interpretation of DTI experiments. For example, a basic step in quantifying diffusion is the calculation of mean eigenvalues of the tensor over repeated measures in a pixel, or across pixels in a homogeneous region of interest (ROI). Typically, this is accomplished by diagonalizing each independent measure of the tensor and averaging the corresponding eigenvalues. However, to perform this calculation some rule must be used to identify the corresponding eigenvalues in the independent measurements. At high signal-to-noise ratio (SNR) this is trivial, but otherwise noise perturbs the eigenvalues, making misclassification more likely. Pierpaoli and Basser (12) used Monte Carlo simulations to show that sorting eigenvalues by magnitude leads to an overestimate of the highest eigenvalue and an underestimate of the lower eigenvalue. This in turn leads to an overestimate of diffusion anisotropy. Hence, the difference between eigenvalues in an isotropic system can appear to be statistically significant. Other studies have used imaging experiments and/or simulations to evaluate the sensitivity of various anisotropy measures to noise (13,14). Using eigenvector information (15) or a combination of eigenvalues and eigenvectors in a dyadic tensor (16) can reduce the sorting bias significantly. However, in anisotropic systems a bias persists even after averaging over a hypothetical, infinitely large ROI (16). The effects of noise on fiber tracking have also been studied using numerical simulations (17–19).

This study uses perturbation theory to evaluate the effects of noise when the sorting procedure is perfect (i.e., corresponding principal axes are correctly identified). The effects of noise on eigenvalues and eigenvectors are found first for the case of asymmetric diffusion (three distinct eigenvalues). Systems with symmetry (both isotropic and axially symmetric diffusion) are considered next. The formalism is used to show that the eigenvalue bias can be reduced by a factor of $1/N$ when combining N independent measurements of the diffusion tensor. The eigenvector noise is then evaluated for an axially symmetric system and the implications of this for MR fiber tracking are discussed. Finally, predictions of the theory are compared to Monte Carlo simulations.

THEORY

The dependence of the NMR signal on the diffusion tensor in a pulsed gradient spin echo (PGSE) experiment depends on the weighting matrix, $\tilde{b}$, according to the relation (1):

$$S(\tilde{b}) = S_0 \exp(-\sum_{i,j=1}^{3} b_{ij} D_{ij}) \qquad [1]$$

where the D_{ij} are elements of the diffusion tensor, $\tilde{D}$, and the b_{ij} are elements of the weighting matrix, given by (20):

$$b_{ij} = \gamma^2 G_i G_j \delta^2 \left(\Delta - \frac{\delta}{3} \right)$$

in the case that gradient ramp times can be ignored and cross terms (21) are insignificant or explicitly cancelled (22). In this expression, G_i is the gradient pulse amplitude in the i^{th} direction ($G_1 = G_x$, etc.), δ is the pulse duration,

Departments of Diagnostic Radiology and Applied Physics, Yale University, New Haven, Connecticut.

*Correspondence to: Adam W. Anderson, Ph.D., Diagnostic Radiology, Yale University School of Medicine, 333 Cedar Street, Fitkin F10, New Haven, CT 06510. E-mail: adam.anderson@yale.edu

Received 18 August 2000; revised 23 May 2001; accepted 18 June 2001.

Δ the interval between rising edges of the two pulses, and γ the gyromagnetic ratio. The direction in which gradients are applied can be described by a unit (column) vector $\hat{r} = (r_1 r_2 r_3)^T$ (T is the transpose operator). If $G_0 = (G_1^2 + G_2^2 + G_3^2)^{1/2}$ is the magnitude of the gradient pulse, then $G_i = r_i G_0$ and:

$$b_{ij} = r_i r_j \cdot \gamma^2 G_0^2 \delta^2 \left(\Delta - \frac{\delta}{3} \right). \quad [2]$$

Summing over diagonal elements, we have:

$$\mathrm{tr}(\tilde{b}) = \gamma^2 G_0^2 \delta^2 \left(\Delta - \frac{\delta}{3} \right) \quad [3]$$

which is equivalent to the b factor of the scalar diffusion coefficient measurement (23). Combining Eqs. [2] and [3], the matrix elements are $b_{ij} = r_i r_j \cdot \mathrm{tr}(\tilde{b})$. Substituting into Eq. [1], one finds:

$$S(\tilde{b}) = S_0 e^{-\mathrm{tr}(\tilde{b}) \cdot \hat{r}^T \tilde{D} \hat{r}} \quad [4]$$

which shows explicitly how signal depends on gradient orientation and the scalar weighting factor, $\mathrm{tr}(\tilde{b})$. In the absence of noise, the diffusion tensor can be determined accurately by fitting Eq. [4]. If noise is significant, however, the tensor determined from measurements of $S(\tilde{b})$ will differ from the true diffusion tensor. Here and below, we will distinguish the measured tensor, $\tilde{D}$, from its true value, $\tilde{D}_0$. In this case, Eq. [4] should be replaced by:

$$S(\tilde{b}) = S_0 e^{-\mathrm{tr}(\tilde{b}) \cdot \hat{r}^T \tilde{D}_0 \hat{r}} + \eta. \quad [5]$$

It is assumed that the noise, η, is independent of $\tilde{b}$ and is normally distributed with mean zero and variance σ_η^2. Hence, the statistical expectation value of $S(\tilde{b})$ is:

$$\langle S(\tilde{b}) \rangle = S_0 e^{-\mathrm{tr}(\tilde{b}) \cdot \hat{r}^T \tilde{D}_0 \hat{r}}.$$

Taking the logarithm of both sides of Eq. [5] and defining $y = \ln(S)$ and $y_0 = \ln(S_0)$, one finds:

$$y(\tilde{b}) = y_0 - \mathrm{tr}(\tilde{b}) \cdot \hat{r}^T \tilde{D}_0 \hat{r} + \ln\left(1 + \frac{\eta}{\langle S(\tilde{b}) \rangle} \right)$$

$$= y_0 - \mathrm{tr}(\tilde{b}) \cdot \hat{r}^T \tilde{D}_0 \hat{r} + \frac{\eta}{\langle S(\tilde{b}) \rangle} - \frac{1}{2} \left(\frac{\eta}{\langle S(\tilde{b}) \rangle} \right)^2 + \ldots . \quad [6]$$

If we neglect terms second order and higher in $\varepsilon \equiv \eta / \langle S(\tilde{b}) \rangle$, then:

$$y(\tilde{b}) = y_0 - \mathrm{tr}(\tilde{b}) \cdot \hat{r}^T \tilde{D}_0 \hat{r} + \varepsilon. \quad [7]$$

In this case, the $y(\tilde{b})$ are normally distributed with mean $\langle y(\tilde{b}) \rangle = y_0 - \mathrm{tr}(\tilde{b}) \cdot \hat{r}^T \tilde{D}_0 \hat{r}$ and variance:

$$\sigma_\varepsilon^2 = \sigma_\eta^2 / \langle S(\tilde{b}) \rangle^2 \quad [8]$$

which depends on $\tilde{b}$. Fitting $y(\tilde{b})$ provides an estimate, $\tilde{D}$, of the true tensor (1).

Perturbation Expansion

Here stationary state perturbation theory (24) is used to find the effects of errors in $\tilde{D}$ on the calculated eigenvalues and eigenvectors. The measured diffusion tensor, $\tilde{D}$, is related to the true tensor, $\tilde{D}_0$, by:

$$\tilde{D} = \tilde{D}_0 + \tilde{V} \quad [9]$$

where $\tilde{V}$ is a random, symmetric matrix. If the matrix elements of the perturbation $\tilde{V}$ are small, then the eigenvalues can be expanded in a power series. The form of the expansion depends on the magnitude of the perturbation relative to the smallest difference between the eigenvalues of $\tilde{D}_0$. If the matrix elements of $\tilde{V}$ are all small compared to the eigenvalue differences, then the system is considered to be nondegenerate. If, on the other hand, the matrix elements of $\tilde{V}$ are comparable to or larger than the eigenvalue differences, the system is degenerate and the approximation must be modified.

Nondegenerate Case

In the simplest case, the three eigenvalues are distinct and the eigenvectors form an orthonormal basis in three dimensions. An eigenvalue and the corresponding eigenvector together define an eigenstate of the system. For state i, the eigenvalue and eigenvector can be expanded in power series:

$$\lambda_i = \lambda_{i0} + \lambda_{i1} + \lambda_{i2} + \ldots$$

$$\mathbf{v}_i = \mathbf{v}_{i0} + \mathbf{v}_{i1} + \mathbf{v}_{i2} + \ldots \quad [10]$$

where λ_{i0} and $\mathbf{v}_{i0}$ are the eigenvalue and eigenvector, respectively, in the case of zero noise and therefore are independent of $\tilde{V}$. λ_{i1} and $\mathbf{v}_{i1}$ are the first-order corrections to the eigenvalue and eigenvector, i.e., they depend on $\tilde{V}$ to first order. Similarly, λ_{i2} and $\mathbf{v}_{i2}$ are the second-order corrections and depend on $\tilde{V}$ to second order. The vectors $\mathbf{v}_i$, etc., are considered column vectors; the corresponding row vectors are given by $\mathbf{v}_i^T$.

Calculation of the terms on the right-hand side of Eq. [10] is straightforward for low orders (details are given in Appendix A). The first-order correction to eigenvalue i is:

$$\lambda_{i1} = \mathbf{v}_{i0}^T \tilde{V} \mathbf{v}_{i0} \quad [11]$$

which is the perturbation evaluated in the unperturbed eigenstate (principal axis direction). The eigenvectors are normalized to all orders, so the perturbations represent changes in orientation rather than magnitude. Hence, the first-order correction is orthogonal to the unperturbed eigenvector:

$$\mathbf{v}_{i0}^T \cdot \mathbf{v}_{i1} = 0. \quad [12]$$

Its projection onto the other two eigenvectors is given by:

$$\mathbf{v}_{j0}^T \cdot \mathbf{v}_{i1} = \frac{\mathbf{v}_{j0}^T \tilde{V} \mathbf{v}_{i0}}{\lambda_{i0} - \lambda_{j0}} \quad (i \neq j). \qquad [13]$$

This implies that the eigenvector $\mathbf{v}_i$ is rotated from the true eigenvector $\mathbf{v}_{i0}$ by angle:

$$\varphi_k \approx \frac{\mathbf{v}_{j0}^T \tilde{V} \mathbf{v}_{i0}}{\lambda_{i0} - \lambda_{j0}} \quad (i \neq j \neq k) \qquad [14]$$

around $\mathbf{v}_k$ (see Appendix A). According to Eqs. [11] and [13], when evaluated in the eigenbasis of $\tilde{D}_0$, the diagonal matrix elements of $\tilde{V}$ give the eigenvalue shifts and the off-diagonal matrix elements give the eigenvector errors to first order. These equations have been derived by Hext (25) using a different approach.

The second-order correction to the eigenvalues is given by:

$$\lambda_{i2} = \sum_{\substack{k=1 \\ (k \neq i)}}^{3} \frac{(\mathbf{v}_{k0}^T \tilde{V} \mathbf{v}_{i0})^2}{\lambda_{i0} - \lambda_{k0}}. \qquad [15]$$

This eigenvalue shift is due to the first-order eigenvector rotation. The perturbation adds a small contribution to $\mathbf{v}_i$ from the other axes, according to Eq. [13]. The second-order correction in Eq. [15] represents the contribution of this small admixture of other states to the shift of λ_i. Note that states of lower diffusivity ($\lambda_{k0} < \lambda_{i0}$) contribute a positive correction, and states of higher diffusivity ($\lambda_{k0} > \lambda_{i0}$) contribute a negative correction (distinct states 'repel' each other in the second order shift). In particular, the net shift is always positive for the highest diffusivity and always negative for the lowest diffusivity. First and second-order corrections to eigenvalues and eigenvectors are shown schematically in Fig. 1.

For a given perturbation $\tilde{V}$, the first and second-order eigenvalue corrections are given by Eqs. [11] and [15]. Suppose that the diffusion tensor is measured N times, each measurement producing three eigenvalues. On average, the eigenvalues will be shifted by the expectation values of the expressions given above. The expectation value of the first order shift is:

$$\langle \lambda_{i1} \rangle = \mathbf{v}_{i0}^T \langle \tilde{V} \rangle \mathbf{v}_{i0}$$

$$= 0 \qquad [16]$$

since we assume the perturbation has zero mean. Hence, the first-order correction vanishes. The expectation value of the second order shift is:

$$\langle \lambda_{i2} \rangle = \sum_{\substack{k=1 \\ (k \neq i)}}^{3} \frac{\langle (\mathbf{v}_{k0}^T \tilde{V} \mathbf{v}_{i0})^2 \rangle}{\lambda_{i0} - \lambda_{k0}}. \qquad [17]$$

The contribution of state k to the second-order shift is simply the ratio of the mean square perturbation matrix element to the difference in diffusivities of the two states. Combining Eqs. [17], [16], and [10], we find that to second order the diffusivities are given by:

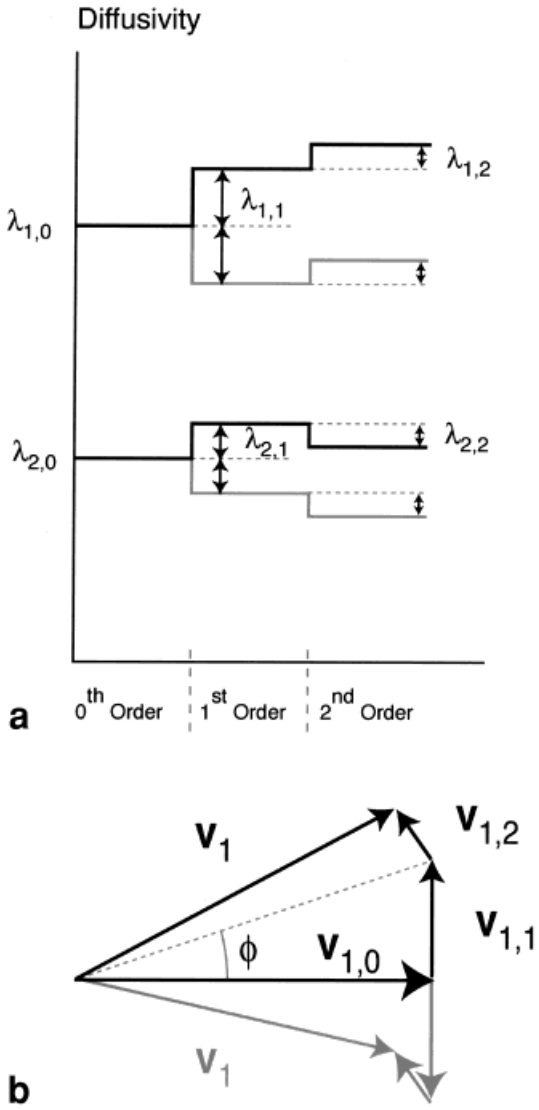

FIG. 1. The effects of a single perturbation, $\tilde{V}$, on the eigenvalues and eigenvectors of the diffusion tensor. First and second-order eigenvalue shifts are shown in **a** for a hypothetical two-dimensional system. The effects of $\tilde{V}$ (in black) and $-\tilde{V}$ (in gray) for each state are opposite in the first-order correction, but are identical in the second order. The second-order shifts of the two states are equal and opposite; the higher state is shifted up, while the lower state is shifted down. First and second-order eigenvector errors are shown in **b.** Perturbations of opposite sign produce the opposite first-order error, but the same second-order error (effects of $\tilde{V}$ are shown in black, those of $-\tilde{V}$ are in gray). For a symmetric distribution of perturbations, the first-order eigenvalue and eigenvector errors average to zero, but the second-order errors have non-zero mean.

$$\langle \lambda_i \rangle = \lambda_{i0} + \sum_{\substack{k=1 \\ (k \neq i)}}^{3} \frac{\langle (\mathbf{v}_{k0}^T \tilde{V} \mathbf{v}_{i0})^2 \rangle}{\lambda_{i0} - \lambda_{k0}}. \qquad [18]$$

Note that the bias increases as the off-diagonal elements of the perturbation increase. For given matrix elements, the bias is larger when the unperturbed eigenvalues are closer together. If the eigenvalues of two or all three states are so close that their differences are not much larger than the

perturbation, then the expansion fails and the states must be considered degenerate.

Degenerate Case

If two or three eigenvalues are the same, then any linear combination of the corresponding eigenvectors is also an eigenvector (with the same eigenvalue). We are free to choose any eigenbasis within the subspace corresponding to the degenerate eigenvalues (such a subspace will also be referred to as a level). The most convenient choice diagonalizes the perturbation. Hence, the q^{th} eigenvector in the space corresponding to the eigenvalue λ_{j0} is written $\mathbf{v}_{j0}^{q}$ and:

$$\mathbf{v}_{j0}^{pT}\tilde{V}\mathbf{v}_{j0}^{q} = \varepsilon_{j}^{q} \cdot \delta_{pq}$$

where ε_{j}^{q} is an eigenvalue of $\tilde{V}$ in this level and δ_{pq} is the Kronecker delta. The power series expansions of the eigenvalues and eigenvectors corresponding to Eq. [10] are:

$$\lambda_{i}^{q} = \lambda_{i0} + \lambda_{i1}^{q} + \lambda_{i2}^{q} + \ldots$$

$$\mathbf{v}_{i}^{q} = \mathbf{v}_{i0}^{q} + \mathbf{v}_{i1}^{q} + \mathbf{v}_{i2}^{q} + \ldots . \qquad [19]$$

The calculation of the terms on the right are analogous to those of the nondegenerate case and are outlined in Appendix B.

The first-order correction to the eigenvalue λ_{i}^{q} is:

$$\lambda_{i1}^{q} = \mathbf{v}_{j0}^{qT}\tilde{V}\mathbf{v}_{i0}^{q}$$

$$= \varepsilon_{i}^{q} \qquad [20]$$

that is, the corresponding eigenvalue of the perturbation matrix. The second-order correction is:

$$\lambda_{i2}^{q} = \sum_{\substack{j=1 \\ (j\neq i)}}^{3} \sum_{p=1}^{n_j} \frac{(\mathbf{v}_{j0}^{pT}\tilde{V}\mathbf{v}_{i0}^{q})^2}{\lambda_{i0} - \lambda_{j0}} \qquad [21]$$

where n_j is the degeneracy (number of dimensions) of level j. The second order shift depends on the matrix elements of the perturbation between the state i and all states with different zero order eigenvalue. Notice that this expression gives the second-order shift of a nondegenerate level, Eq. [15], as a special case ($n_i = 1$, $n_j = 1$ or 2). Since Eq. [21] covers both degenerate and nondegenerate cases, it can be used to show that the sum of the second-order shifts of all states is zero (see Appendix C):

$$\sum_{i=1}^{3} \sum_{q=1}^{n_i} \lambda_{i2}^{q} = 0. \qquad [22]$$

To evaluate the expectation value of the first-order shift, assume that the probability density function, $P(\tilde{V})$, for the perturbation satisfies:

$$P(\tilde{V}) = P(-\tilde{V})$$

that is, the perturbation is symmetrically distributed around zero. This condition is satisfied by the multivariate (zero-mean) normal distribution, for example. Since $\tilde{V}$ and $-\tilde{V}$ share eigenvectors but have eigenvalues of opposite sign, the expectation value of Eq. [20] represents the integral of an odd function over the entire six-dimensional space of perturbations. This symmetry requires that:

$$\langle \lambda_{i1}^{q} \rangle = 0. \qquad [23]$$

Taking expectation values of both sides of Eq. [21] yields:

$$\langle \lambda_{i2}^{q} \rangle = \sum_{\substack{j=1 \\ (j\neq i)}}^{3} \sum_{p=1}^{n_j} \frac{\langle (\mathbf{v}_{j0}^{pT}\tilde{V}\mathbf{v}_{i0}^{q})^2 \rangle}{\lambda_{i0} - \lambda_{j0}}.$$

Combining this result with Eq. [23] in Eq. [19] yields:

$$\langle \lambda_{i}^{q} \rangle = \lambda_{i0} + \sum_{\substack{j=1 \\ (j\neq i)}}^{3} \sum_{p=1}^{n_j} \frac{\langle (\mathbf{v}_{j0}^{pT}\tilde{V}\mathbf{v}_{i0}^{q})^2 \rangle}{\lambda_{i0} - \lambda_{j0}}. \qquad [24]$$

Taking the expectation value of Eq. [22] shows that the sum of the eigenvalues is unbiased. Hence, measurements of the trace of the diffusion tensor are unbiased to second order.

For diffusion in three dimensions, Eq. [24] can be simplified because the degenerate space can have only two or three dimensions. In the case of a three-dimensional degenerate space (isotropic diffusion), there is only one state ($i = 1$), and no other state j to couple to, so the shift is zero:

$$\langle \lambda_{1}^{1} \rangle = \langle \lambda_{1}^{2} \rangle = \langle \lambda_{1}^{3} \rangle = \lambda_{1,0}. \qquad [25]$$

If the degenerate space has two dimensions (axially symmetric diffusion), then there is only one state ($j = 2$) to couple to and it is nondegenerate ($n_j = 1$). In this case, Eq. [24] reduces to:

$$\langle \lambda_{1}^{q} \rangle = \lambda_{1,0} + \frac{\langle (\mathbf{v}_{2,0}^{T}\tilde{V}\mathbf{v}_{1,0}^{q})^2 \rangle}{\lambda_{1,0} - \lambda_{2,0}}.$$

If the degeneracy is not exact, but the level splittings (eigenvalue differences) are not all large compared to the perturbations, then this formalism can still be used. In this case, $\tilde{D}_0$ can be split into two parts: $\tilde{D}_{00}$ in which the closely spaced levels are exactly degenerate and $\tilde{D}_{01}$ which produces the small level splitting. The second part, $\tilde{D}_{01}$, can be added to the perturbation and the analysis carried forward in a straightforward way. In this case the expected first-order shift of the 'degenerate' levels will not be zero, but will be given by the matrix elements of $\tilde{D}_{01}$.

Averaging Tensor Measurements

If the means of the principal diffusivities are desired in a region of interest (ROI), averaging can be done at any of three steps of the calculation. First, the NMR signal can be averaged across pixels in the ROI, and the average signal fitted to find the elements of the tensor, which can then be

diagonalized. Second, the diffusion tensor can be calculated separately in each pixel and the average of these tensors can be diagonalized. Third, the eigenvalues of $\tilde{D}$ can be found in each pixel and these can be averaged. The purpose of this section is to compare the eigenvalue bias inherent in each of these strategies and to show that the third option, although commonly used, leads to the largest bias.

Averaging the NMR signal over N pixels in a homogeneous ROI, the analog of Eq. [6] is:

$$\ln(\bar{S}(\tilde{b})) = y_0 - \mathrm{tr}(\tilde{b}) \cdot \hat{r}^T \tilde{D}_0 \hat{r} + \frac{\bar{\eta}}{\langle S(\tilde{b}) \rangle} + \ldots$$

where bars indicate ROI averages and $\sigma^2_{\bar{\eta}} = \sigma^2_\eta / N$ if the noise in different voxels is independent. Averaging the N measurements of $S(\tilde{b})$ reduces the noise variance by the factor $1/N$. This decreases the mean squared perturbation matrix elements (in Eqs. [18] and [24]), and hence the eigenvalue bias by the factor $1/N$ (see Appendix D).

In the second method, the diffusion tensor is calculated separately in each pixel, then averaged prior to diagonalization. In this case, the true diffusion tensor is estimated by the mean of N measurements.

$$\bar{\tilde{D}} = \frac{1}{N} \sum_{n=1}^{N} \tilde{D}_n \qquad [26]$$

where $\tilde{D}_n$ is the diffusion tensor on the n^{th} measurement. If $\tilde{V}_n$ is the random perturbation on the n^{th} measurement, then $\tilde{D}_n = \tilde{D}_0 + \tilde{V}_n$, and:

$$\bar{\tilde{D}} = \tilde{D}_0 + \bar{\tilde{V}} \qquad [27]$$

where $\bar{\tilde{V}}$ is the mean perturbation matrix:

$$\bar{\tilde{V}} = \frac{1}{N} \sum_{n=1}^{N} \tilde{V}_n. \qquad [28]$$

The mean perturbation affects the eigenvalues of the mean tensor in exactly the same way that the individual perturbations, $\tilde{V}_n$, affect the eigenvalues of $\tilde{D}_n$. Hence, if $\bar{\lambda}_i$ is an eigenvalue of $\bar{\tilde{D}}$, then by analogy to Eq. [18],

$$\langle \bar{\lambda}_i \rangle = \lambda_{i0} + \sum_{\substack{k=1 \\ (k \neq i)}}^{3} \frac{\langle (\mathbf{v}_{k0}^T \bar{\tilde{V}} \mathbf{v}_{i0})^2 \rangle}{\lambda_{i0} - \lambda_{k0}} \qquad [29]$$

assuming the unperturbed tensor is uniform over the ROI. Since the $\tilde{V} = \tilde{V}_n$ are independent,

$$\langle (\mathbf{v}_{k0}^T \bar{\tilde{V}} \mathbf{v}_{i0})^2 \rangle = \langle (\mathbf{v}_{k0}^T \tilde{V} \mathbf{v}_{i0})^2 \rangle / N \qquad [30]$$

Eq. [29] becomes:

$$\langle \bar{\lambda}_i \rangle = \lambda_{i0} + \frac{1}{N} \cdot \sum_{\substack{k=1 \\ (k \neq i)}}^{3} \frac{\langle (\mathbf{v}_{k0}^T \tilde{V} \mathbf{v}_{i0})^2 \rangle}{\lambda_{i0} - \lambda_{k0}}$$

$$= \lambda_{i0} + \frac{\langle \lambda_{i2} \rangle}{N} \qquad [31]$$

for the nondegenerate case, and using Eq. [24]:

$$\langle \bar{\lambda}_i^q \rangle = \lambda_{i0}^q + \frac{1}{N} \sum_{j \neq i} \sum_{p=1}^{n_j} \frac{\langle (\mathbf{v}_{j0}^{pT} \tilde{V}_n \mathbf{v}_{i0}^q)^2 \rangle}{\lambda_{i0} - \lambda_{j0}}$$

$$= \lambda_{i0}^q + \frac{\langle \lambda_{i2}^q \rangle}{N} \qquad [32]$$

for a degenerate level. Note that this is the same decrease in bias obtained by averaging the signal over the ROI, prior to fitting for the diffusion tensor.

The third strategy of calculating the eigenvalues in each pixel, then averaging these over the ROI gives the bias found in Eq. [18] (nondegenerate case) or Eq. [24] (degenerate case). Since both the first and second strategies reduce the bias by a factor $1/N$ compared to this method, they are preferable. Another advantage of the first two strategies is that they avoid the complications of eigenvalue sorting.

Implications for MR Fiber Tracking

Although eigenvalue bias is a larger concern for conventional DTI, eigenvector noise has greater impact on MR fiber tracking. As a specific example, consider the case of axially symmetric diffusion, with the largest diffusivity along the symmetry axis. This is the simplest model of diffusion in white matter axon bundles in the brain. Labeling the fast diffusion axis with the index $i = 1$, the corresponding eigenvector is:

$$\mathbf{v}_1 = \mathbf{v}_{1,0} + \sum_{j=2}^{3} \left(\frac{\mathbf{v}_{j0}^T \tilde{V} \mathbf{v}_{1,0}}{\lambda_{1,0} - \lambda_{j0}} \right) \mathbf{v}_{j0} \qquad [33]$$

to first order. Note that Eq. [13] has been used since the fast diffusion level is nondegenerate (any eigenvector basis can be chosen in the degenerate space perpendicular to $\mathbf{v}_1$).

In its simplest form, fiber tracking rests on the assumption that $\mathbf{v}_1$ identifies the local tangent to a fiber. Hence, beginning at point $\mathbf{R}$ in space, another point along the path can be found at $\mathbf{R} \pm a\mathbf{v}_1$, where a is the step size (assumed to be small compared to the local radius of curvature of the fiber). This process can be repeated, moving in both directions from the initial point, until some termination criterion is met (e.g., the anisotropy of $\tilde{D}$ falls below a threshold value). The difference between $\mathbf{v}_1$ and the true eigenvector, $\mathbf{v}_{1,0}$, represents a limit to the accuracy of the fiber paths generated this way.

Assuming that $\tilde{D}_0$ is spatially invariant, its eigenvector basis $\{\mathbf{v}_{1,0}, \mathbf{v}_{2,0}, \mathbf{v}_{3,0}\}$ can be chosen to be spatially invariant. Let the coordinates of a point relative to this basis be (x_1, x_2, x_3). Ideally, a fiber path beginning at the origin

satisfies $x_2 = x_3 = 0$ at all points along the path. However, because $\mathbf{v}_1$ differs from $\mathbf{v}_{1,0}$, the coordinates x_2 and x_3 will be non-zero generally. For example, the component of $\mathbf{v}_1$ in the direction of $\mathbf{v}_{2,0}$ is, using Eq. [33],

$$\mathbf{v}_{2,0}^T \cdot \mathbf{v}_1 \approx \frac{\mathbf{v}_{2,0}^T \tilde{V} \mathbf{v}_{1,0}}{\lambda_{1,0} - \lambda_{2,0}}$$

so a step of length a along $\mathbf{v}_1$ corresponds to an increment in x_2 given by:

$$\delta x_2 \approx a \cdot \frac{\mathbf{v}_{2,0}^T \tilde{V} \mathbf{v}_{1,0}}{\lambda_{1,0} - \lambda_{2,0}}.$$

Since $\tilde{V}$ varies randomly from voxel to voxel, the calculated fiber path executes a random walk around the $\mathbf{v}_{1,0}$ axis. After N_s steps, the x_2 displacement is:

$$x_2 \approx a \cdot \sum_{n=1}^{N_s} \frac{\mathbf{v}_{2,0}^T \tilde{V}_n \mathbf{v}_{1,0}}{\lambda_{1,0} - \lambda_{2,0}}$$

where $\tilde{V}_n$ is the perturbation for the n^{th} step. The expectation value of x_2 is:

$$\langle x_2 \rangle \approx a \cdot \sum_{n=1}^{N_s} \frac{\mathbf{v}_{2,0}^T \langle \tilde{V}_n \rangle \mathbf{v}_{1,0}}{\lambda_{1,0} - \lambda_{2,0}}$$

$$\approx 0$$

to first order, but the mean squared value is:

$$\langle x_2^2 \rangle \approx a^2 \cdot \left\langle \sum_{n=1}^{N_s} \frac{\mathbf{v}_{2,0}^T \tilde{V}_n \mathbf{v}_{1,0}}{\lambda_{1,0} - \lambda_{2,0}} \cdot \sum_{p=1}^{N_s} \frac{\mathbf{v}_{2,0}^T \tilde{V}_p \mathbf{v}_{1,0}}{\lambda_{1,0} - \lambda_{2,0}} \right\rangle$$

$$\approx a^2 \cdot \sum_{n=1}^{N_s} \sum_{p=1}^{N_s} \frac{\langle \mathbf{v}_{2,0}^T \tilde{V}_n \mathbf{v}_{1,0} \cdot \mathbf{v}_{2,0}^T \tilde{V}_p \mathbf{v}_{1,0} \rangle}{(\lambda_{1,0} - \lambda_{2,0})^2}.$$

Suppose the step size, a, is chosen to be a particular fraction of the voxel width w:

$$a = \frac{w}{M}$$

for integer M. There is only one sample of $\tilde{V}$ per voxel, so if steps n and p are in the same voxel $\tilde{V}_p = \tilde{V}_n$, but otherwise the perturbations are uncorrelated. The correlation of the perturbation between steps can be accounted for with the following approximation. For each n, we assume that $\tilde{V}_p = \tilde{V}_n$ for an average of M values of p (i.e., M steps), and no correlation exists for other p. In this case,

$$\langle x_2^2 \rangle \approx a^2 M \cdot \sum_{n=1}^{N_s} \frac{\langle (\mathbf{v}_{2,0}^T \tilde{V}_n \mathbf{v}_{1,0})^2 \rangle}{(\lambda_{1,0} - \lambda_{2,0})^2}.$$

Similarly, each value of $\tilde{V}_n$ is repeated an average of M times in the sum. If each voxel that the fiber path travels through is given an index m, then the summation can be rewritten as:

$$\langle x_2^2 \rangle \approx a^2 M^2 \cdot \sum_{m=1}^{N_v} \frac{\langle (\mathbf{v}_{2,0}^T \tilde{V}_m \mathbf{v}_{1,0})^2 \rangle}{(\lambda_{1,0} - \lambda_{2,0})^2}$$

where the $\tilde{V}_m$ are independent random matrices, and N_V is the number of voxels traversed by the path. Since the $\tilde{V}_m$ are sampled from the same distribution,

$$\langle x_2^2 \rangle \approx a^2 M^2 N_V \cdot \frac{\langle (\mathbf{v}_{2,0}^T \tilde{V} \mathbf{v}_{1,0})^2 \rangle}{(\lambda_{1,0} - \lambda_{2,0})^2}$$

$$\approx w^2 N_V \cdot \frac{\langle (\mathbf{v}_{2,0}^T \tilde{V} \mathbf{v}_{1,0})^2 \rangle}{(\lambda_{1,0} - \lambda_{2,0})^2}.$$

The root-mean-square (RMS) deviation of the calculated path from the true path is then:

$$(x_2)_{\text{RMS}} \approx w \frac{(\mathbf{v}_{2,0}^T \tilde{V} \mathbf{v}_{1,0})_{\text{RMS}}}{\lambda_{1,0} - \lambda_{2,0}} \cdot \sqrt{N_V}. \quad [34]$$

This has the usual form for a random walk: the RMS displacement is equal to the step size times the square root of the number of steps. Note that the effective step size along the fiber is the voxel width, since this is the correlation length of the perturbation.

In order for the RMS path error to be less than the voxel width, Eq. [34] implies:

$$\frac{\lambda_{1,0} - \lambda_{2,0}}{(\mathbf{v}_{2,0}^T \tilde{V} \mathbf{v}_{1,0})_{\text{RMS}}} > \sqrt{N_V}. \quad [35]$$

The term on the left-hand side can be interpreted loosely as the diffusivity contrast-to-noise ratio (CNR) in the fiber voxels. According to this relation, accurate fiber tracking requires that the diffusivity CNR be at least as large as the square root of the fiber length (measured in voxels). An analogous expression gives the RMS displacement in the $\mathbf{v}_{3,0}$ direction.

From a practical point of view it is more useful to express Eq. [35] in terms of the noise variance, which can be estimated directly from an image. The off-diagonal matrix elements of the perturbation are related to the SNR of an unweighted ($\tilde{b} = 0$) image by:

$$\langle (\mathbf{v}_{j0}^T \tilde{V} \mathbf{v}_{i0})^2 \rangle = \left(\frac{\sigma_\eta}{S_0} \right)^2 \cdot (\tilde{R} [\tilde{X}^T \tilde{W} \tilde{X}]^{-1} \tilde{R}^T)_{i+j+2, i+j+2} \quad (i \neq j) \quad [36]$$

where $\tilde{X}$ is the design matrix for multivariate linear regression, $\tilde{W}$ is a diagonal weighting matrix, and $\tilde{\text{R}}$ transforms the noise covariance matrix to the principal axis coordinate frame of $\tilde{D}_0$ (see Appendix D). Substituting this relation into Eq. [35], one finds:

$$\frac{S_0}{\sigma_n} > \frac{\sqrt{N_V \cdot (\tilde{R}[\tilde{X}^T\tilde{W}\tilde{X}]^{-1}\tilde{R}^T)_{55}}}{\lambda_{1,0} - \lambda_{2,0}}. \quad [37]$$

This relation defines the minimum SNR required for accurate fiber tracking using simple algorithms. Image SNR can be improved by increasing voxel size, up to the point that partial volume averaging becomes significant in fiber voxels. Alternatively, SNR can be increased by averaging repeated measures. For given fiber diameter (which sets voxel size), length (which sets N_V), and diffusion contrast ($\lambda_{1,0} - \lambda_{2,0}$), Eq. [37] determines the minimum SNR, and hence imaging time, required for accurate tracking.

NUMERICAL SIMULATION

Monte Carlo simulations were used to estimate the effects of noise on calculated diffusion tensor eigenvalues. Signal amplitude was calculated (according to Eq. [5]) using three values of diffusion weighting, $\mathrm{tr}(\tilde{b}) = 0$, 500, and 1000 s/mm^2, the non-zero values applied in six directions:

$$\hat{r}^T = \begin{cases} (1, 0, 0) \\ (0, 1, 0) \\ (0, 0, 1) \\ \frac{1}{\sqrt{2}}(1, 1, 0) \\ \frac{1}{\sqrt{2}}(1, 0, 1) \\ \frac{1}{\sqrt{2}}(0, 1, 1) \end{cases}.$$

The true diffusion tensor, $\tilde{D}_0$, was chosen to be isotropic, axially symmetric, or asymmetric. In each case, the mean diffusivity, $\lambda_{\mathrm{mean}} \equiv \mathrm{tr}(\tilde{D}_0)/3$, was chosen to approximate that found in the human brain ($\lambda_{\mathrm{mean}} = 0.7 \times 10^{-3}$ mm^2/s). For the two anisotropic cases, the range of diffusivities, $\lambda_{\max} - \lambda_{\min}$, was chosen to be $\lambda_{\mathrm{mean}}/2$ and the true eigenvectors lay along the x, y, and z directions.

Complex noise was calculated from two (zero mean) Gaussian random variables, x and y, and added in quadrature, $z = x + iy$. The standard deviation of the noise was the same in each channel, $\sigma_x = \sigma_y = \sigma$. The noise was added to the ideal (real) signal and the magnitude of the sum represented the measured signal. This calculation was performed for each of 13 measurements (six gradient directions at two non-zero amplitudes, plus an unweighted image) for each of $n = 25$ pixels in a hypothetical, uniform ROI. Components of the diffusion tensor in each pixel were then determined by a weighted least-squares fit of $\ln(S)$ as a function of the elements b_{ij}. All calculations were performed in MATLAB (MathWorks, Natick, MA).

The eigenvalues and eigenvectors of a tensor have no inherent ordering. The order established by a particular numerical routine depends on the algorithm employed and the precise values of the tensor components. For example, very low levels of noise can lead to a reordering of the calculated eigenvalues and eigenvectors, even though the eigenvalues and eigenvectors themselves are modified only slightly. Therefore some care must be taken in averaging eigenvalues (or eigenvectors) across independent measurements, as in the different pixels in an ROI. The calculated mean values will depend on how corresponding eigenvalues are identified in different pixels, i.e., on how they are sorted. In the simulation, ROI-averaged diffusivities were calculated in three ways. First, the tensor in each pixel was diagonalized and the eigenvalues were assigned to the variable $\lambda_{\max}$, λ_{mid} or $\lambda_{\min}$ according to magnitude. This will be referred to as magnitude sorting. Second, the mean tensor, $\bar{\tilde{D}}$, in the ROI was calculated. Eigenvalues of the individual pixel tensors were then sorted by maximizing the similarity to the mean tensor, using the dyadic tensor overlap statistic (16):

$$C_t = \frac{\sum_{i=1}^{3} \lambda_i \bar{\lambda}_i (\mathbf{v}_i^T \bar{\mathbf{v}}_i)^2}{\sum_{i=1}^{3} \lambda_i \bar{\lambda}_i}$$

or the analogous expression for the degenerate case (tensor sorting). This involves testing the six possible mappings of the eigenvalues (and eigenvectors) of one tensor onto those of the other and choosing the pairing that produces the largest value of C_t. This is intended to identify the best match between the two diffusion ellipsoids. The pixel eigenvalues, λ_i, assigned to each mean tensor eigenvalue, $\bar{\lambda}_i$, were then averaged to find the mean over the ROI. Third, the eigenvalues of the mean tensor $\bar{\tilde{D}}$ were calculated directly. This will be referred to as the mean tensor calculation. This approach does not explicitly sort eigenvalues from individual pixels, but averages the diagonal elements of the individual tensors in a common reference frame. The alternate method of averaging the signal over the ROI prior to fitting and diagonalizing is equivalent to the mean tensor calculation under the conditions used here and so was not tested independently.

Each of the procedures above produced three average eigenvalues for the ROI. In order to make a precise estimate of their expectation values, the process was repeated until 10^4 samples were generated for each eigenvalue and method. Again, some procedure must be chosen to match the eigenvalues across samples. Magnitude sorting was used to find the mean values of the (ROI-averaged) $\lambda_{\max}$, λ_{mid}, and $\lambda_{\min}$. Tensor sorting was used to find the mean values for the two remaining methods.

The predictions of Eqs. [18] and [31] (or Eqs. [24] and [32] for the degenerate case) were tested by evaluating the off-diagonal elements of the perturbation matrix. The mean-squared matrix elements were calculated over all pixels and samples. At moderate and high SNR and the relatively large eigenvalue differences used here, the tensor sorting algorithm is expected to perform with near-perfect accuracy. Hence, Eq. [18] (or Eq.[24]) should agree with the ROI averages obtained by tensor sorting. In addition, Eq. [31] (or Eq. [32]) should agree with the ROI averages obtained by the mean tensor calculation. The theory does not apply to magnitude sorting, which was simulated for comparison only.

To determine the accuracy of the predictions at various SNR levels, the entire procedure was repeated for several

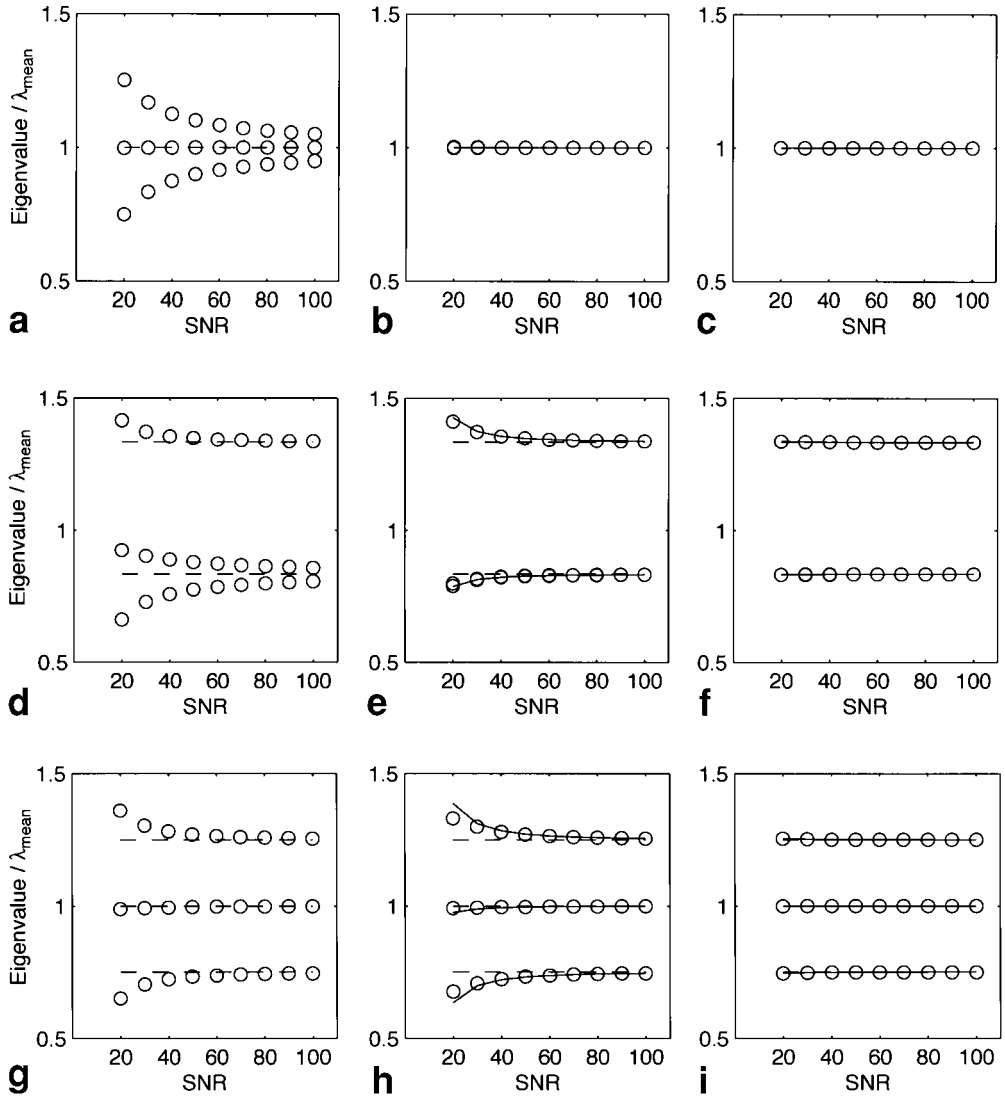

FIG. 2. Estimated ROI eigenvalues as functions of SNR for isotropic diffusion (top row, subplots **a, b, c**), axially symmetric diffusion (middle row, subplots **d, e, f**), and asymmetric diffusion (bottom row, subplots **g, h, i**). ROI averages were calculated using magnitude sorting (left column, subplots **a, d, g**), tensor sorting (middle column, subplots **b, e, h**), and mean tensor calculations (right column, subplots **c, f, i**). The lower lines in **e** and **f** represent the two degenerate states, which have nearly the same eigenvalues. True eigenvalues are displayed as dashed lines. Predictions of second-order perturbation theory are shown as solid lines. Pixel-by-pixel tensor sorting produces less bias than magnitude sorting and the mean tensor calculation improves on both other methods. Second-order perturbation theory correctly predicts the bias when the ratio of the perturbation matrix elements to the eigenvalue splittings are much less than one. Standard errors of the mean values are smaller than the plotting symbols, and are not shown.

values of σ. SNR was defined as the maximum (i.e., unweighted) signal, S_0, divided by the standard deviation of the noise, σ. The simulation was performed for SNR values from 20 to 100 (in steps of 10).

A similar approach was used to evaluate the effects of noise on fiber tracking and to compare these to the predictions of the theory. Diffusion was assumed to be axially symmetric around $\hat{x}$, with:

$$\lambda_{10} - \lambda_{20} = \lambda_{10} - \lambda_{30} = \lambda_{mean}/2.$$

All paths started from the origin. At each step, noise was added to the ideal signal for the 13 measurements described above and the eigenvectors of the resulting diffusion tensor were determined. To minimize sorting errors, the eigenvectors (and eigenvalues) were sorted according to their similarity to the true diffusion tensor (using the tensor sorting algorithm). A new path position was calculated by stepping a fixed distance (one voxel width) along $\mathbf{v}_1$, the eigenvector corresponding to the fast diffusion axis. This procedure was repeated for a total of 256 steps for each fiber. The x_2 and x_3 coordinates of the path, both zero ideally, were determined as a function of step number. The calculation was carried out for 10^4 fibers and the mean and standard deviation of the path errors were found. The entire procedure was performed for SNR values 35, 50, and 70. Otherwise, the parameters of the simulation were the same as in the eigenvalue bias simulation.

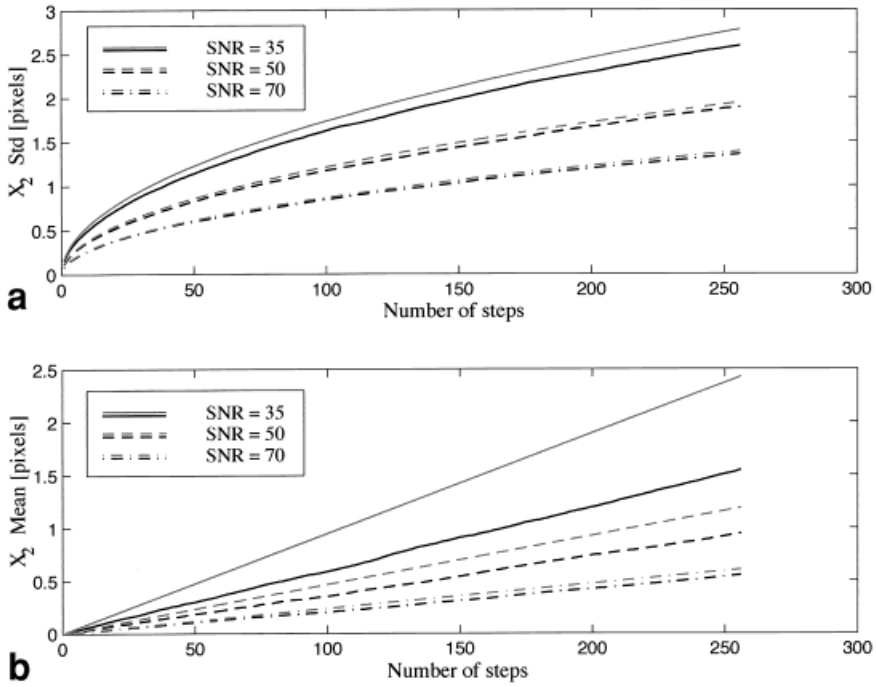

FIG. 3. Track error as a function of step number. Errors in eigenvector orientation produce position errors in fiber tracks. Theoretical predictions (in gray) and Monte Carlo simulations (in black) are shown for SNR = 35, 50, and 70. The standard deviation of track positions (**a**) increases with the square root of step number and the standard deviation of image noise (the lines for SNR = 70 nearly coincide). The mean error (**b**) is proportional to step number and (at higher SNR) the variance of image noise. Results for the x_3 axis are the same.

RESULTS AND DISCUSSION

The mean eigenvalues in the simulated ROI are shown in Fig. 2 for the cases of isotropic, axisymmetric, and asymmetric diffusion. The true eigenvalues and the predictions of the perturbation expansion are also shown. For isotropic diffusion (full degeneracy), magnitude sorted eigenvalues demonstrate a strong bias: $\lambda_{\max}$ is greater and $\lambda_{\min}$ is less than the true principal diffusivity. λ_{mid} is not biased by sorting. On the other hand, eigenvalues estimated by pixel-by-pixel tensor sorting and the mean tensor calculation show almost no bias at these SNR levels. (All three methods have a small bias at the lowest SNR due to the nonlinear logarithmic transformation). For anisotropic diffusion (the axially symmetric and asymmetric cases), all three methods produce biased estimates of the eigenvalues. For the parameters chosen here, the bias for pixel-by-pixel tensor sorting is somewhat less than that of magnitude sorting. The bias of the mean tensor calculation is significantly less than both other methods.

The theoretical predictions overestimate the bias where it is largest. In the worst case (asymmetric diffusion, subplot *h*) at the lowest SNR value (SNR = 20), the bias of the highest diffusivity is overestimated by 70%. Low precision is expected in this case, however. The second-order approximation used to make the prediction is based on the assumption that the ratios:

$$\alpha_{ik} \equiv \frac{\mathbf{v}_{k0}^T \tilde{V} \mathbf{v}_{i0}}{\lambda_{i0} - \lambda_{k0}} \qquad [38]$$

are small compared to unity. For the point in question, the standard deviations of the α_{ik} are as large as $(\sigma_\alpha)_{\max} = 0.6$, so values of α_{ik} on the order of unity are likely. In this case, higher-order terms in the perturbation expansion cannot be discarded. At higher SNR, the second-order approximation is justified (since $(\sigma_\alpha)_{\max}$ scales as SNR^{-1}). For the corresponding point at SNR = 50 we have $(\sigma_\alpha)_{\max} = 0.25$ and the predicted bias of the largest eigenvalue equals the tensor sorted value to within 7% (the eigenvalues agree to 0.1%). At each SNR the theoretical prediction agrees better with the mean tensor calculation than the tensor sorted value, since in the former case α_{ik} *is* $N^{-1/2} = 0.2$ times the value on the right-hand side of Eq. [38].

The mean tensor calculation performs better than pixel-by-pixel tensor sorting because it takes greater advantage of multiple measures. The eigenvalues of the mean tensor equal the mean values of the diagonal elements of the individual tensors, evaluated in the diagonal frame of the mean tensor. By averaging tensor elements in a common coordinate frame, the effects of noise average out for large *N*. Averaging eigenvalues, rather than tensors, amounts to averaging tensor elements in different coordinate frames, which leads to biased estimates even for infinitely many independent measurements. In general, it is better to average tensors then diagonalize, than it is to diagonalize tensors then average. However, averaging tensors offers no better reduction in bias than averaging the diffusion-weighted signal in the ROI prior to fitting for the tensor components. (In fact, at low SNR calculations based on the average signal will have better noise immunity than the mean tensor calculation.) The same arguments apply to 'time domain averaging,' which involves repeated measures of the diffusion tensor in a given pixel (14). The relations in Eqs. [31] and [32] apply to this method as well, if *N* is taken to be the number of repeated measurements. Hence, time domain averaging reduces the bias of pixel-by-pixel tensor sorting by $1/N$. However, the same gain is realized simply by averaging the diffusion weighted signal across acquisitions prior to fitting.

These relations imply the following stratification. At low SNR, bias is minimized by averaging the NMR signal across repeated measures prior to fitting for tensor components. At moderate SNR ($\alpha_{ik} \ll 1$), averaging across individually determined tensors is equally effective. Only at high SNR (where α_{ik} is negligible) is eigenvalue averaging equivalent to the other methods.

The effect of image noise on fiber paths is shown in Fig. 3. The standard deviation of track errors is shown in Fig. 3a as a function of step number. Results of Monte Carlo simulations are compared to the predictions of Eq. [34]. The simulation results follow the expected square root dependence on step number. However, the theoretical predictions overestimate the effects of noise at lower SNR. According to the first-order theory, the standard deviation of track errors scales as σ_η (i.e., as SNR^{-1}); however, the actual errors increase more slowly with increasing noise.

According to perturbation theory, the mean track error in each step is zero to first order, but is generally non-zero in second order. For the simulated system, the mean is the same for each step, so the error accumulates over many steps to produce a small but significant track deviation. This is shown in Fig. 3b. The mean error is proportional to step number and (nearly) doubles when the noise increases by a factor of $\sqrt{2}$ at higher SNR (e.g., going from SNR = 70 to SNR = 50). The latter result supports the prediction that the mean error is second order in the noise. Again, the theory overestimates the effect of noise: the second-order prediction (based on Eq. [50] of Appendix A) overestimates the simulated value by 16% at SNR = 70 and by 53% at SNR = 35.

The theoretical predictions for both the mean and standard deviation of track error overestimate the true displacements because the tensor sorting procedure limits eigenvector errors (i.e., when eigenvectors are rotated sufficiently by noise, the sorting procedure relabels them to preserve the best match to the unperturbed tensor). The simple theory presented here would predict that eigenvector components have normal distributions, but in fact the tails of these distributions are truncated by sorting (and by normalization). Since the largest deviations are missing from the distributions, the actual track displacements are smaller than predicted. As SNR increases, the distributions become more Gaussian and the theory fits the simulation results more closely. This affects the second-order calculation more, since this depends on higher-order moments of the distribution of errors. While the theory overestimates the simulated errors somewhat, the latter are calculated using the value of the true tensor. In practical situations the true tensor is not known, so the sorting used in the simulation represents an ideal case. Fiber tracks generated without this information may have larger position errors.

More sophisticated methods of fiber reconstruction may have better noise immunity than the simple scheme analyzed here. Tracking methods that regularize, or smooth, fiber tangent information have been shown to reduce the cumulative effects of eigenvector noise (17,26). Hence, if the minimum SNR defined in Eq. [37] is not available (at the desired resolution in a reasonable scan time), then some form of regularization is required to maintain path accuracy. Note that although regularization reduces the first-order errors in path position, it cannot address the path bias due to the mean second order eigenvector errors. Fortunately, these terms are expected to be small (for moderate to high SNR).

Apart from quantitative predictions of eigenvalue and eigenvector errors, the theory presented here should aid in understanding general features of DTI measurements, e.g., the functional dependence of these errors on image SNR and diffusion contrast. As a specific example, the spatial coherence of 'fast axis' eigenvectors, $\mathbf{v}_1$, can be a useful indication of white matter integrity (8). A straightforward interpretation of this quantity relates it to the similarity of fiber orientations in neighboring voxels. However, changes in the spatial coherence of $\mathbf{v}_1$ should be interpreted with caution, since the coherence also depends on eigenvector noise. According to Eq. [14], eigenvector errors can vary even if image noise is constant, since these errors depend on eigenvalue contrast as well. Hence, pathology that makes diffusion more isotropic would be expected to decrease eigenvector coherence, without any changes in the distribution of fiber orientations.

Similarly, some care should be taken in interpreting the SNR values given for this and other studies of the effects of noise. For a given physical system, the effects of noise on eigenvalues and eigenvectors are determined by the matrix elements of the perturbation. How these are related to the noise level, σ_η, depends on the values of $\tilde{b}$ used in an experiment (i.e., on the design matrix, $\tilde{X}$). For example, discarding the intermediate value of $\mathrm{tr}(\tilde{b})$ used here would increase the eigenvalue bias at the same SNR level. Alternatively, for the same number of measurements the bias could be reduced at each SNR by using any of several better optimized encoding schemes (27–29). Hence, the diffusion encoding scheme (and precise definition of SNR) must be taken into account when comparing the SNR dependence found in different studies.

As a final note, it may seem contradictory to carry the perturbation expansion in Eq. [10] to second order after dropping second and higher order terms in Eq. [6]. However, the expansion parameters in these power series are different and are expected to have different magnitudes. In Eq. [6] we neglect terms second order in $\eta/\langle S(\tilde{b})\rangle$, which is of order 1/SNR. In Eq. [10], we retain terms second order in α_{ik}. We assume that $\alpha_{ik} \ll 1$ and $\mathrm{SNR} \gg 1$, but allow for the case that $\alpha_{ik} > 1/\mathrm{SNR}$. The assumption of moderate to high SNR in unweighted images is meant to guarantee that $\alpha_{ik} \ll 1$. This condition is not particularly restrictive but may require signal averaging across repeated acquisitions to improve image SNR.

CONCLUSIONS

At moderate and high SNR, a power series expansion of the eigenvalues and eigenvectors of the diffusion tensor can be used to study the effects of noise. These effects include a shift in eigenvalues that is independent of sorting bias. Second-order perturbation theory accurately predicts the bias found by Monte Carlo simulation. When averaging the results of several independent measurements, the bias is reduced by averaging individual tensors prior to diagonalization, or by averaging the signal prior to fitting for the tensor components. In addition, eigenvector

noise leads to a random walk of calculated trajectories in simple fiber tracking schemes and may represent a fundamental limit to accuracy. More generally, the formalism described here can be used to estimate the contribution of noise to experimental results and to optimize the trade-off between SNR and resolution in DTI studies.

ACKNOWLEDGMENTS

The author thanks Z. Ding and J.C. Gore for helpful discussions.

APPENDIX A

Equation [10] implies that the inner product of $\mathbf{v}_{j0}$ and $\mathbf{v}_i$ is:

$$\mathbf{v}_{j0}^T \cdot \mathbf{v}_i = \delta_{ij} + \mathbf{v}_{j0}^T \cdot \mathbf{v}_{i1} + \mathbf{v}_{j0}^T \cdot \mathbf{v}_{i2} + \ldots . \quad [39]$$

The eigenvectors are required to be orthonormal to all orders, that is:

$$\mathbf{v}_j^T \cdot \mathbf{v}_i = \delta_{ij}. \quad [40]$$

Since the eigenvectors span the three-dimensional space, we have the completeness relation:

$$\sum_{k=1}^{3} \mathbf{v}_{k0} \cdot \mathbf{v}_{k0}^T = 1. \quad [41]$$

Inserting this into Eq. [40] yields:

$$\sum_{k=1}^{3} (\mathbf{v}_j^T \cdot \mathbf{v}_{k0})(\mathbf{v}_{k0}^T \cdot \mathbf{v}_i) = \delta_{ij}.$$

Substituting Eq. [39] in both terms in the sum,

$$\sum_{k=1}^{3} (\delta_{jk} + \mathbf{v}_{j1}^T \cdot \mathbf{v}_{k0} + \mathbf{v}_{j2}^T \cdot \mathbf{v}_{k0} + \ldots)$$

$$\times (\delta_{ik} + \mathbf{v}_{k0}^T \cdot \mathbf{v}_{i1} + \mathbf{v}_{k0}^T \cdot \mathbf{v}_{i2} + \ldots) = \delta_{ij}$$

$$\sum_{k=1}^{3} \delta_{jk}\delta_{ik} + \sum_{k=1}^{3} (\delta_{jk}\mathbf{v}_{k0}^T \cdot \mathbf{v}_{i1} + \mathbf{v}_{j1}^T \cdot \mathbf{v}_{k0}\delta_{ik})$$

$$+ \sum_{k=1}^{3} (\delta_{jk}\mathbf{v}_{k0}^T \cdot \mathbf{v}_{i2} + \mathbf{v}_{j1}^T \cdot \mathbf{v}_{k0}\mathbf{v}_{k0}^T \cdot \mathbf{v}_{i1} + \mathbf{v}_{j2}^T \cdot \mathbf{v}_{k0}\delta_{ik}) = \delta_{ij}.$$

In the second equality, terms of the same order have been grouped together. This equation holds for arbitrary (but small) noise levels, so it must hold separately for each order. Setting the zero order terms on both sides to be equal, we get the identity $\delta_{ij} = \delta_{ij}$. For the first-order terms, we find:

$$\sum_{k=1}^{3} (\delta_{jk}\mathbf{v}_{k0}^T \cdot \mathbf{v}_{i1} + \mathbf{v}_{j1}^T \cdot \mathbf{v}_{k0}\delta_{ik}) = 0$$

$$\mathbf{v}_{j0}^T \cdot \mathbf{v}_{i1} + \mathbf{v}_{j1}^T \cdot \mathbf{v}_{i0} = 0.$$

Choosing $i = j$, the two terms on the left are the transpose of one another. Since they are both scalars, they must be equal, so:

$$\mathbf{v}_{i0}^T \cdot \mathbf{v}_{i1} = 0. \quad [42]$$

Hence, the first-order correction to an eigenvector is orthogonal to the zero-order eigenvector. Evaluating the second-order terms for $i = j$ gives,

$$\mathbf{v}_{i0}^T \cdot \mathbf{v}_{i2} = -\frac{1}{2} \sum_{k=1}^{3} (\mathbf{v}_{k0}^T \cdot \mathbf{v}_{i1})^2. \quad [43]$$

The eigenvalue equation for the perturbed diffusion tensor is:

$$\tilde{D}\mathbf{v}_i = \lambda_i \mathbf{v}_i.$$

Inserting the completeness relation Eq. [41] on the left, and multiplying both sides of the resulting equation by $\mathbf{v}_{j0}^T$ from the left yields:

$$\sum_{k=1}^{3} \mathbf{v}_{j0}^T \tilde{D} \mathbf{v}_{k0} \mathbf{v}_{k0}^T \cdot \mathbf{v}_i = \lambda_i \mathbf{v}_{j0}^T \cdot \mathbf{v}_i.$$

Substituting Eq. [9] for the diffusion tensor and Eq. [10] for the eigenvector and eigenvalue, we find:

$$\sum_{k=1}^{3} \mathbf{v}_{j0}^T (\tilde{D}_0 + \tilde{V}) \mathbf{v}_{k0} (\delta_{ik} + \mathbf{v}_{k0}^T \cdot \mathbf{v}_{i1} + \mathbf{v}_{k0}^T \cdot \mathbf{v}_{i2} + \ldots)$$

$$= (\lambda_{i0} + \lambda_{i1} + \lambda_{i2} + \ldots)(\delta_{ij} + \mathbf{v}_{j0}^T \cdot \mathbf{v}_{i1} + \mathbf{v}_{j0}^T \cdot \mathbf{v}_{i2} + \ldots). \quad [44]$$

Again, terms of the same order on the left and right sides of the equation are equal. Hence, the zero-order terms give:

$$\sum_{k=1}^{3} \mathbf{v}_{j0}^T \tilde{D}_0 \mathbf{v}_{k0} \delta_{ik} = \lambda_{i0} \delta_{ij}$$

$$\lambda_{i0}\delta_{ij} = \lambda_{i0}\delta_{ij}$$

since the $\mathbf{v}_{k0}$ are eigenvectors of $\tilde{D}_0$. Equating the first-order terms gives:

$$\sum_{k=1}^{3} (\mathbf{v}_{j0}^T \tilde{D}_0 \mathbf{v}_{k0} \mathbf{v}_{k0}^T \cdot \mathbf{v}_{i1} + \mathbf{v}_{j0}^T \tilde{V} \mathbf{v}_{k0} \delta_{ik}) = \lambda_{i0} \mathbf{v}_{j0}^T \cdot \mathbf{v}_{i1} + \lambda_{i1} \delta_{ij}$$

$$(\lambda_{j0} - \lambda_{i0}) \mathbf{v}_{j0}^T \cdot \mathbf{v}_{i1} + \mathbf{v}_{j0}^T \tilde{V} \mathbf{v}_{i0} = \lambda_{i1} \delta_{ij}. \quad [45]$$

Setting $i = j$ gives the first-order correction to the eigenvalues:

$$\lambda_{i1} = \mathbf{v}_{i0}^T \tilde{V} \mathbf{v}_{i0}. \quad [46]$$

The first-order shift of the eigenvalue equals the perturbation evaluated in the unperturbed eigenstate (principal axis direction). For $i \neq j$, Eq. [45] gives:

$$\mathbf{v}_{j0}^T \cdot \mathbf{v}_{i1} = \frac{\mathbf{v}_{j0}^T \tilde{V} \mathbf{v}_{i0}}{\lambda_{i0} - \lambda_{j0}} \quad (i \neq j). \quad [47]$$

Equation [42] shows that the first-order correction to the eigenvectors is orthogonal to the zero-order eigenvector of the same state. Equation [47] gives the projection of the correction onto the other axes. The eigenvector $\mathbf{v}_i$ is rotated from the true eigenvector $\mathbf{v}_{i0}$ by angle:

$$\varphi_k \approx \varepsilon_{ijk} \cdot \frac{\mathbf{v}_{j0}^T \tilde{V} \mathbf{v}_{i0}}{\lambda_{i0} - \lambda_{j0}}$$

around $\mathbf{v}_k$. φ_k is the right-handed rotation angle around $\mathbf{v}_k$, with $\varepsilon_{ijk} = 1$ if ijk is an even permutation of 123, $\varepsilon_{ijk} = -1$ if ijk is an odd permutation of 123, and $\varepsilon_{ijk} = 0$ otherwise.

Equating the second-order terms on the right and left sides of Eq. [44],

$$\sum_{k=1}^{3} (\mathbf{v}_{j0}^T \tilde{D}_0 \mathbf{v}_{k0} \mathbf{v}_{k0}^T \cdot \mathbf{v}_{i2} + \mathbf{v}_{j0}^T \tilde{V} \mathbf{v}_{k0} \mathbf{v}_{k0}^T \cdot \mathbf{v}_{i1})$$

$$= \lambda_{i0} \mathbf{v}_{j0}^T \cdot \mathbf{v}_{i2} + \lambda_{i1} \mathbf{v}_{j0}^T \cdot \mathbf{v}_{i1} + \lambda_{i2} \delta_{ij}$$

$$(\lambda_{j0} - \lambda_{i0}) \mathbf{v}_{j0}^T \cdot \mathbf{v}_{i2} + \sum_{k=1}^{3} \mathbf{v}_{j0}^T \tilde{V} \mathbf{v}_{k0} \mathbf{v}_{k0}^T \cdot \mathbf{v}_{i1} = \lambda_{i1} \mathbf{v}_{j0}^T \cdot \mathbf{v}_{i1} + \lambda_{i2} \delta_{ij}. \quad [48]$$

Setting $i = j$ and using Eq. [42] gives the second-order correction for the eigenvalues:

$$\lambda_{i2} = \sum_{k=1}^{3} \mathbf{v}_{i0}^T \tilde{V} \mathbf{v}_{k0} \mathbf{v}_{k0}^T \cdot \mathbf{v}_{i1}$$

$$= \sum_{\substack{k=1 \\ (k \neq i)}}^{3} \frac{(\mathbf{v}_{k0}^T \tilde{V} \mathbf{v}_{i0})^2}{\lambda_{i0} - \lambda_{k0}} \quad [49]$$

where Eq. [47] was used to get the second equality. The second-order correction to state i is $\tilde{V}$ evaluated between the zeroth-order eigenvector and the admixture of the other eigenvectors, produced by the perturbation.

One component of the second-order correction to the eigenvectors is given by Eq. [43]. The remaining components are obtained by evaluating Eq. [48] for $i \neq j$ and using Eqs. [46] and [47], which yields:

$$\mathbf{v}_{j0}^T \cdot \mathbf{v}_{i2} = -\frac{\mathbf{v}_{i0}^T \tilde{V} \mathbf{v}_{i0} \cdot \mathbf{v}_{j0}^T \tilde{V} \mathbf{v}_{i0}}{(\lambda_{j0} - \lambda_{i0})^2} + \sum_{k \neq i} \frac{\mathbf{v}_{j0}^T \tilde{V} \mathbf{v}_{k0}}{\lambda_{j0} - \lambda_{i0}} \cdot \frac{\mathbf{v}_{k0}^T \tilde{V} \mathbf{v}_{i0}}{\lambda_{k0} - \lambda_{i0}} \quad (i \neq j). \quad [50]$$

This is the second-order contribution to the eigenvector orientation error.

APPENDIX B

For degenerate levels, the projection of $\mathbf{v}_i^q$ onto $\mathbf{v}_{j0}^p$ is, according to Eq. [19],

$$\mathbf{v}_{j0}^{pT} \cdot \mathbf{v}_i^q = \delta_{ji} \delta_{pq} + \mathbf{v}_{j0}^{pT} \cdot \mathbf{v}_{i1}^q + \mathbf{v}_{j0}^{pT} \cdot \mathbf{v}_{i2}^q + \ldots . \quad [51]$$

The completeness relation in the degenerate case is:

$$\sum_{j=1}^{3} \sum_{p=1}^{n_j} \mathbf{v}_{j0}^p \cdot \mathbf{v}_{j0}^{pT} = 1 \quad [52]$$

where n_j is the degeneracy of the j^{th} eigenvalue. The normalization condition for the perturbed eigenvectors is:

$$\mathbf{v}_k^{rT} \cdot \mathbf{v}_i^q = \delta_{ki} \delta_{rq}.$$

Inserting Eq. [52] into the left side, and using Eq. [51], we can solve the equation separately for each order. The first order equation requires that:

$$\mathbf{v}_{i0}^{qT} \cdot \mathbf{v}_{i1}^q = 0.$$

As in the nondegenerate case, the first-order correction to an eigenvector is perpendicular to the unperturbed axis.

The eigenvalue equation is:

$$\tilde{D} \mathbf{v}_i^q = \lambda_i^q \cdot \mathbf{v}_i^q. \quad [53]$$

Inserting Eq. [52] on the left side of this relation and projecting both sides onto $\mathbf{v}_{k0}^r$ yields:

$$\sum_{j,p} (\mathbf{v}_{k0}^{rT} \tilde{D} \mathbf{v}_{j0}^p)(\mathbf{v}_{j0}^{pT} \cdot \mathbf{v}_i^q) = \lambda_i^q (\mathbf{v}_{k0}^{rT} \cdot \mathbf{v}_i^q).$$

Substituting Eqs. [9], [51], and the top equality in Eq. [19], we can again solve the equation one order at a time. The zero order equation is an identity, as in the nondegenerate case. The first-order equation is:

$$(\lambda_{k0} - \lambda_{i0}) \mathbf{v}_{k0}^{rT} \cdot \mathbf{v}_{i1}^q + \mathbf{v}_{k0}^{rT} \tilde{V} \mathbf{v}_{i0}^q = \lambda_{i1}^q \cdot \delta_{ik} \delta_{qr}. \quad [54]$$

For $k = i$ and $r = q$, this becomes:

$$\lambda_{i1}^q = \mathbf{v}_{i0}^{qT} \tilde{V} \mathbf{v}_{i0}^q$$

$$= \varepsilon_i^q. \quad [55]$$

Hence, the first-order shift is an eigenvalue of the perturbation matrix. For $k \neq i$, Eq. [54] reduces to:

$$\mathbf{v}_{k0}^{rT}\cdot\mathbf{v}_{i1}^{q}=\frac{\mathbf{v}_{k0}^{rT}\tilde{V}\mathbf{v}_{i0}^{q}}{\lambda_{i0}-\lambda_{k0}}\quad(i\neq k)$$

which gives the components (in the unperturbed coordinate frame) of the first-order corrections to the eigenvectors. The second-order equation yields the eigenvalue correction:

$$\lambda_{i2}^{q}=\sum_{\substack{j=1\\(j\neq i)}}^{3}\sum_{p=1}^{n_j}\frac{(\mathbf{v}_{j0}^{pT}\tilde{V}\mathbf{v}_{i0}^{q})^2}{\lambda_{i0}-\lambda_{j0}}. \qquad [56]$$

APPENDIX C

Writing Eq. [56] for the most general case (non- or mixed degeneracy) and summing over states in all levels gives:

$$\sum_{i=1}^{3}\sum_{q=1}^{n_i}\lambda_{i2}^{q}=\sum_{i=1}^{3}\sum_{q=1}^{n_i}\sum_{\substack{j=1\\(j\neq i)}}^{3}\sum_{p=1}^{n_j}\frac{(\mathbf{v}_{j0}^{pT}\tilde{V}\mathbf{v}_{i0}^{q})^2}{\lambda_{i0}-\lambda_{j0}}.$$

The sum on the right can be broken into terms for $i>j$ and $i<j$:

$$\sum_{i=1}^{3}\sum_{q=1}^{n_i}\lambda_{i2}^{q}=\sum_{i=1}^{3}\sum_{q=1}^{n_i}\sum_{j=1}^{i-1}\sum_{p=1}^{n_j}\frac{(\mathbf{v}_{j0}^{pT}\tilde{V}\mathbf{v}_{i0}^{q})^2}{\lambda_{i0}-\lambda_{j0}}+\sum_{i=1}^{3}\sum_{q=1}^{n_i}\sum_{j=i+1}^{3}\sum_{p=1}^{n_j}\frac{(\mathbf{v}_{j0}^{pT}\tilde{V}\mathbf{v}_{i0}^{q})^2}{\lambda_{i0}-\lambda_{j0}}$$

where terms like $\Sigma_{j=1}^{0}$ are understood to be zero. Interchanging the order of summation in the second term on the right gives:

$$\sum_{i=1}^{3}\sum_{q=1}^{n_i}\lambda_{i2}^{q}=\sum_{i=1}^{3}\sum_{q=1}^{n_i}\sum_{j=1}^{i-1}\sum_{p=1}^{n_j}\frac{(\mathbf{v}_{j0}^{pT}\tilde{V}\mathbf{v}_{i0}^{q})^2}{\lambda_{i0}-\lambda_{j0}}+\sum_{j=1}^{3}\sum_{p=1}^{n_j}\sum_{i=1}^{j-1}\sum_{q=1}^{n_i}\frac{(\mathbf{v}_{j0}^{pT}\tilde{V}\mathbf{v}_{i0}^{q})^2}{\lambda_{i0}-\lambda_{j0}}.$$

The index labels are arbitrary; exchanging the labels i and j (and p and q) in the second term on the right gives:

$$\sum_{i=1}^{3}\sum_{q=1}^{n_i}\lambda_{i2}^{q}=\sum_{i=1}^{3}\sum_{q=1}^{n_i}\sum_{j=1}^{i-1}\sum_{p=1}^{n_j}\frac{(\mathbf{v}_{j0}^{pT}\tilde{V}\mathbf{v}_{i0}^{q})^2}{\lambda_{i0}-\lambda_{j0}}+\sum_{i=1}^{3}\sum_{q=1}^{n_i}\sum_{j=1}^{i-1}\sum_{p=1}^{n_j}\frac{(\mathbf{v}_{j0}^{qT}\tilde{V}\mathbf{v}_{j0}^{p})^2}{\lambda_{j0}-\lambda_{i0}}$$

$$=\sum_{i=1}^{3}\sum_{q=1}^{n_i}\sum_{j=1}^{i-1}\sum_{p=1}^{n_j}\left\{\frac{(\mathbf{v}_{j0}^{pT}\tilde{V}\mathbf{v}_{i0}^{q})^2}{\lambda_{i0}-\lambda_{j0}}+\frac{(\mathbf{v}_{i0}^{qT}\tilde{V}\mathbf{v}_{j0}^{p})^2}{\lambda_{j0}-\lambda_{i0}}\right\}=0$$

since $\mathbf{v}_{j0}^{pT}\tilde{V}\mathbf{v}_{i0}^{q}$ is a scalar, and hence equals its transpose. The last result is Eq. [22].

APPENDIX D

Multivariate linear regression provides an estimate, $\tilde{D}$, of the true tensor, $\tilde{D}_0$, based on a set of diffusion-weighted measurements (1). Equation [7] can be written for an entire set of measurements by arranging the values of $y(\tilde{b})$ and the error ε in column vector form (one row per measurement). These are denoted by $\vec{y}$ and $\vec{\varepsilon}$, respectively. Similarly, the unknown quantities, $y_0=\ln(S_0)$ and the elements of the diffusion tensor, can be arranged in a column vector $\vec{\beta}_0$:

$$\vec{\beta}_0=\begin{pmatrix}y_0\\(\tilde{D}_0)_{11}\\(\tilde{D}_0)_{22}\\(\tilde{D}_0)_{33}\\(\tilde{D}_0)_{12}\\(\tilde{D}_0)_{13}\\(\tilde{D}_0)_{23}\end{pmatrix}. \qquad [57]$$

In terms of these vectors, Eq. [7] can be written:

$$\vec{y}=\tilde{X}\cdot\vec{\beta}_0+\vec{\varepsilon} \qquad [58]$$

where each row of the design matrix, $\tilde{X}$, has the form:

$$(1\quad -b_{11}\quad -b_{22}\quad -b_{33}\quad -2b_{12}\quad -2b_{13}\quad -2b_{23})$$

and the values in row n depend on the $\tilde{b}$ matrix for the nth measurement. The weighted least-squares solution to Eq. [58] is:

$$\vec{\beta}=(\tilde{X}^T\tilde{\Sigma}_\varepsilon^{-1}\tilde{X})^{-1}\cdot\tilde{X}^T\tilde{\Sigma}_\varepsilon^{-1}\cdot\vec{y} \qquad [59]$$

where $\tilde{\Sigma}_\varepsilon$ is the covariance matrix of the error $\vec{\varepsilon}$. The covariance matrix of $\vec{\beta}$ is:

$$\tilde{\Sigma}_\beta=(\tilde{X}^T\tilde{\Sigma}_\varepsilon^{-1}\tilde{X})^{-1}. \qquad [60]$$

Assuming the errors are independent in different measurements, $\tilde{\Sigma}_\varepsilon$ is a diagonal matrix with diagonal elements given by Eq. [8]. Therefore, the inverse of the covariance matrix is also diagonal with elements:

$$(\tilde{\Sigma}_\varepsilon^{-1})_{nn}=\frac{\langle S(\tilde{b}_n)\rangle^2}{\sigma_\eta^2} \qquad [61]$$

where $\tilde{b}_n$ is the $\tilde{b}$ matrix for the n^{th} measurement and σ_η^2 is the noise variance (assumed to be the same in all measurements). Defining a diagonal weighting matrix, $\tilde{W}$, with non-zero elements:

$$\tilde{W}_{nn}\equiv e^{-2\mathrm{tr}(\tilde{b}_n)\cdot\hat{r}_n^T\tilde{D}_0\hat{r}_n}=\left(\frac{\langle S(\tilde{b}_n)\rangle}{S_0}\right)^2 \qquad [62]$$

where $\hat{r}_n$ is the diffusion-weighting direction for measurement n, we have:

$$\tilde{\Sigma}_\varepsilon^{-1} = \left(\frac{S_0}{\sigma_\eta}\right)^2 \tilde{W} \qquad [63]$$

Substituting this relation in Eq. [60], the covariance matrix of the estimated quantities can be written:

$$\tilde{\Sigma}_\beta = \left(\frac{\sigma_\eta}{S_0}\right)^2 \cdot (\tilde{X}^T \tilde{W} \tilde{X})^{-1}. \qquad [64]$$

The first term on the right side reflects the SNR of an unweighted image. The second term depends on the diffusion encoding scheme and the orientation of the principal axes relative to the gradient axes.

The diagonal elements of the covariance matrix $\tilde{\Sigma}_\beta$ give the variance of individual components of $\vec{\beta}$. We have:

$$(\tilde{\Sigma}_\beta)_{ii} = \langle(\vec{\beta} - \vec{\beta}_0)_i^2\rangle. \qquad [65]$$

The last six elements of $(\vec{\beta} - \vec{\beta}_0)$ are the errors in the estimated diffusion tensor components. These are also the elements of the perturbation matrix. According to the ordering convention of Eq. [57], $(\tilde{\Sigma}_\beta)_{11}$ gives the variance of the estimated value of $\ln(S_0)$. The mean square diagonal elements of $\tilde{V}$ are:

$$\langle(\tilde{V}_{ii})^2\rangle = \langle[D_{ii} - (D_0)_{ii}]^2\rangle = (\tilde{\Sigma}_\beta)_{i+1,i+1} \quad (i \le 3) \qquad [66]$$

and the mean square off-diagonal elements are:

$$\langle(\tilde{V}_{ij})^2\rangle = \langle[D_{ij} - (D_0)_{ij}]^2\rangle = (\tilde{\Sigma}_\beta)_{i+j+2,i+j+2} \quad (i, j \le 3;\ i \ne j). \qquad [67]$$

These relations, combined with Eq. [64], give the variance of the perturbation matrix elements in the coordinate system defined by the gradient axes. Terms like $\langle(\mathbf{v}_{j0}^T \tilde{V} \mathbf{v}_{i0})^2\rangle$ are easier to evaluate in the principal axis coordinate system, however. Transforming the covariance matrix $\tilde{\Sigma}_\beta$, the variances of the perturbation matrix elements in the principal axis coordinate frame are:

$$\langle(\tilde{V}_{ii})^2\rangle = (\tilde{R}\tilde{\Sigma}_\beta\tilde{R}^T)_{i+1,i+1} \quad (i \le 3) \qquad [68]$$

and:

$$\langle(\tilde{V}_{ij})^2\rangle = (\tilde{R}\tilde{\Sigma}_\beta\tilde{R}^T)_{i+j+2,i+j+2} \quad (i, j \le 3;\ i \ne j) \qquad [69]$$

where the transformation matrix for the covariance matrix is (25):

$$\tilde{R} = \begin{pmatrix} 1 & 0 & 0 & 0 & 0 & 0 & 0 \\ 0 & v_{10x}^2 & v_{10y}^2 & v_{10z}^2 & 2v_{10x}v_{10y} & 2v_{10x}v_{10z} & 2v_{10y}v_{10z} \\ 0 & v_{20x}^2 & v_{20y}^2 & v_{20z}^2 & 2v_{20x}v_{20y} & 2v_{20x}v_{20z} & 2v_{20y}v_{20z} \\ 0 & v_{30x}^2 & v_{30y}^2 & v_{30z}^2 & 2v_{30x}v_{30y} & 2v_{30x}v_{30z} & 2v_{30y}v_{30z} \\ 0 & v_{10x}v_{20x} & v_{10y}v_{20y} & v_{10z}v_{20z} & v_{10x}v_{20y} + v_{20x}v_{10y} & v_{10x}v_{20z} + v_{20x}v_{10z} & v_{10y}v_{20z} + v_{20y}v_{10z} \\ 0 & v_{10x}v_{30x} & v_{10y}v_{30y} & v_{10z}v_{30z} & v_{10x}v_{30y} + v_{30x}v_{10y} & v_{10x}v_{30z} + v_{30x}v_{10z} & v_{10y}v_{30z} + v_{30y}v_{10z} \\ 0 & v_{20x}v_{30x} & v_{20y}v_{30y} & v_{20z}v_{30z} & v_{20x}v_{30y} + v_{30x}v_{20y} & v_{20x}v_{30z} + v_{30x}v_{20z} & v_{20y}v_{30z} + v_{30y}v_{20z} \end{pmatrix}.$$

For clarity, the x, y, and z components of the eigenvectors have been denoted explicitly. Hence, v_{10x} is the x component (in the gradient frame) of the unperturbed eigenvector v_{10}, and so on. In the principal axis frame, $\mathbf{v}_{j0}^T \tilde{V} \mathbf{v}_{i0} = \tilde{V}_{ji}$, so Eq. [68] can be written:

$$\langle(\mathbf{v}_{i0}^T \tilde{V} \mathbf{v}_{i0})^2\rangle = (\tilde{R}\tilde{\Sigma}_\beta\tilde{R}^T)_{i+1,i+1} \quad (i \le 3) \qquad [70]$$

and Eq. [69] becomes:

$$\langle(\mathbf{v}_{j0}^T \tilde{V} \mathbf{v}_{i0})^2\rangle = (\tilde{R}\tilde{\Sigma}_\beta\tilde{R}^T)_{i+j+2,i+j+2} \quad (i, j \le 3;\ i \ne j). \qquad [71]$$

Equation [70] gives the variance of the first-order shift for nondegenerate eigenvalues (see Eq. [11]). Since the variance of the second-order bias is fourth order in the perturbation, Eq. [70] will describe the total variance of the eigenvalue to a good approximation. Equation [71] gives the numerator in the expression for the mean shift of a nondegenerate level (see Eq. [18]). Note that these relations do not apply to a degenerate level, since in that case the zero-order eigenvectors, and hence the transformation matrix $\tilde{R}$, are also random. Substituting Eq. [64] into Eq. [71], we have:

$$\langle(\mathbf{v}_{j0}^T \tilde{V} \mathbf{v}_{i0})^2\rangle = \left(\frac{\sigma_\eta}{S_0}\right)^2 \cdot (R(\tilde{X}^T \tilde{W} \tilde{X})^{-1} \tilde{R}^T)_{i+j+2,i+j+2} \quad (i \ne j) \qquad [72]$$

which relates the mean squared off-diagonal matrix element to experimental parameters.

REFERENCES

1. Basser PJ, Mattiello J, LeBihan D. Estimation of the effective self-diffusion tensor from the NMR spin echo. J Magn Reson B 1994;103: 247–254.
2. Beaulieu C, Allen PS. Determinants of anisotropic water diffusion in nerves. Magn Reson Med 1994;31:394–400.
3. Beaulieu C, Allen PS. Water diffusion in the giant axon of the squid: implications for diffusion-weighted MRI of the nervous system. Magn Reson Med 1994;32:579–583.
4. Pierpaoli C, Jezzard P, Basser PJ, Barnett A, Di Chiro G. Diffusion tensor imaging of the human brain. Radiology 1996;201:637–648.
5. Buchsbaum MS, Tang CY, Peled S, Gudbjartsson H, Lu D, Hazlett EA, Downhill J, Haznedar M, Fallon JH, Atlas SW. MRI white matter diffu-

sion anisotropy and PET metabolic rate in schizophrenia. Neuroreport 1998;9:425–430.
6. Werring DJ, Clark CA, Barker GJ, Thompson AJ, Miller DH. Diffusion tensor imaging of lesions and normal-appearing white matter in multiple sclerosis. Neurology 1999;52:1626–1632.
7. Werring DJ, Toosy AT, Clark CA, Parker GJ, Barker GJ, Miller DH, Thompson AJ. Diffusion tensor imaging can detect and quantify corticospinal tract degeneration after stroke. J Neurol Neurosurg Psychiatry 2000;69:269–272.
8. Pfefferbaum A, Sullivan EV, Hedehus M, Lim KO, Adalsteinsson E, Moseley M. Age-related decline in brain white matter anisotropy measured with spatially corrected echo-planar diffusion tensor imaging. Magn Reson Med 2000;44:259–268.
9. Basser PJ. Fiber tractography via diffusion tensor MRI (DT-MRI). In: Proc 6th Scientific Meeting ISMRM, Sydney, 1998. p 1226.
10. Xue R, van Zijl PCM, Crain BJ, Solaiyappan M, Mori S. In vivo three-dimensional reconstruction of rat brain axonal projections by diffusion tensor imaging. Magn Reson Med 1999;42:1123–1127.
11. Conturo TE, Lori NF, Cull TS, Akbudak E, Snyder AZ, Shimony JS, McKinstry RC, Burton H, Raichle ME. Tracking neuronal fiber pathways in the living human brain. Proc Natl Acad Sci USA 1999;96:10422–10427.
12. Pierpaoli C, Basser PJ. Toward a quantitative assessment of diffusion anisotropy. Magn Reson Med 1996;36:893–906.
13. Bastin ME, Armitage PA, Marshall I. A theoretical study of the effect of experimental noise on the measurement of anisotropy in diffusion imaging. Magn Reson Imag 1998;16:773–785.
14. Skare S, Li T-Q, Nordell B, Ingvar M. Noise considerations in the determination of diffusion tensor anisotropy. Magn Reson Imag 2000; 18:659–669.
15. Martin KM, Papadakis NG, Huang CL-H, Hall LD, Carpenter TA. The reduction of the sorting bias in the eigenvalues of the diffusion tensor. Magn Reson Imag 1999;17:893–901.
16. Basser PJ, Pajevic S. Statistical artifacts in diffusion tensor MRI (DT-MRI) caused by background noise. Magn Reson Med 2000;44:41–50.
17. Basser PJ, Pajevic S, Pierpaoli C, Duda J, Aldroubi A. In vivo fiber tractography using DT-MRI data. Magn Reson Med 2000;44:625–632.
18. Tournier J-D, Calamante F, King MD, Gadian DG, Connelly A. Limitations and requirements of diffusion tensor fibre-tracking: assessment using simulations. In: Proc 9th Scientific Meeting ISMRM, Glasgow, 2001. p 1521.
19. Lazar M, Hasan KM, Alexander A. Bootstrap analysis of DT-MRI tractography techniques: streamlines and tensorlines. In: Proc 9th Scientific Meeting ISMRM, Glasgow, 2001. p 1527.
20. Mattiello J, Basser PJ, LeBihan D. Analytical expressions for the b matrix in NMR diffusion imaging and spectroscopy. J Magn Reson A 1994;108:131–141.
21. Neeman M, Freyer JP, Sillerud LO. Pulsed-gradient spin-echo diffusion studies in NMR imaging. Effects of the imaging gradients on the determination of diffusion coefficients. J Magn Reson 1990;90:303–312.
22. Neeman M, Freyer JP, Sillerud LO. A simple method for obtaining cross-term-free images for diffusion anisotropy studies in NMR microimaging. Magn Reson Med 1991;21:138–143.
23. Stejskal EO, Tanner JE. Spin diffusion measurements: spin echoes in the presence of a time-dependent field gradient. J Chem Phys 1965;42: 288–292.
24. Corson EM. Perturbation methods in the quantum mechanics of n-electron systems. London: Blackie & Son; 1951. p 75–85.
25. Hext, GR. The estimation of second-order tensors, with related tests and designs. Biometrika 1963;50:353–373.
26. Poupon C, Clark CA, Frouin V, Regis J, Bloch I, Le Bihan D, Mangin J-F. Regularization of diffusion-based direction maps for the tracking of brain white matter fascicles. NeuroImage 2000;12:184–195.
27. Papadakis NG, Xing D, Huang CL-H, Hall LD, Carpenter TA. A comparative study of acquisition schemes for diffusion tensor imaging using MRI. J Magn Reson 1999;137:67–82.
28. Jones DK, Horsfield MA, Simmons A. Optimal strategies for measuring diffusion in anisotropic systems by magnetic resonance imaging. Magn Reson Med 1999;42:515–525.
29. Papadakis NG, Murrills CD, Hall LD, Huang CL-H, Carpenter TA. Minimal gradient encoding for robust estimation of diffusion anisotropy. Magn Reson Imag 2000;18:671–679.